SAND2010-3996C

Designing Metal-Organic Frameworks for Radiation Detection

Patrick L. Feng, Janelle Branson, Khalid, Hattar, Gyorgy Vizkelethy, Mark D. Allendorf, F. Patrick Doty*

Sandia National Laboratories, California
7011 East Ave
Livermore, CA 94550

Sandia National Laboratories, New Mexico
PO Box 5800
Albuquerque, NM 87185

1. Introduction.

The synthesis of improved materials for the detection and identification of subatomic particles is vital for progress in nuclear nonproliferation, space exploration, nuclear power, and other critical applications in the chemical, biological, and medical fields. A crucial requirement to this end is a detailed physical understanding of the factors that affect the efficiency and timing of light output in scintillating materials, including chemical composition, electronic structure, interchromophore interactions, crystalline symmetry, and atomic density. Unfortunately, none of the material types currently used in radiation detection (crystalline inorganic compounds, organic crystals, plastics, liquid scintillators) possess the inherent synthetic flexibility that is necessary for the systematic control and understanding of these factors. Here we investigate the structure-property relationships of five metal-organic framework (MOF)-based scintillators, highlighting the unique advantages of these crystalline and highly tailorable compounds as a platform upon which to design new materials for specific radiation detection applications.

MOFs are periodic 1-D through 3-D crystalline materials comprised of metal clusters linked by coordinating organic groups, whose structures may be predicted and designed through an understanding of the geometric nets accessible for particular metal cluster/linker combinations.[1-3] This extremely high degree of structural versatility , combined with the ability to independently modify the identity of the linker group, further differentiates MOFs from other extended crystalline materials such as zeolites and molecular solids. Thus, it is possible to obtain families of isostructural MOFs comprised of a variety of linker groups, including a multitude of conjugated organic molecules that function as scintillators. A subset of these linkers is depicted in figure 1, illustrating differences with respect to the length and geometric orientation of these connecting groups. MOFs may also possess permanent nanoporosities as a result of the self assembly between linker molecules and metal clusters, enabling them to serve as hosts for wavelength shifters or other elements to improve the scintillating and detection characteristics of the material (e.g. Li or B).

Our group recently reported the first two examples of MOF-based scintillators, both of which are based upon the linker group 4,4'-trans-stilbenedicarboxylic acid (H_2SDC).[4] Significant differences in the photoluminescence and radioluminescence spectra are observed between each MOF structure and single crystals of H_2SDC, including large radioluminescence Stokes' shifts for the MOF structures. These observations were interpreted in terms of the crystal structures and extent of interchromophore coupling, as mediated by pinning of the linker groups to the metal cluster nodes. Here we expand these studies to a series of scintillating MOFs comprised of the linker groups 4,4'-biphenyldicarboxylic acid (H_2BPDC) and 2,6-naphthalenedicarboxylic acid (H_2NDC), illustrating the origin of these large Stokes' shifts and the ability to modify the luminescence via incorporation of extrinsic dopants within the MOF pores.

2. Experimental.

Photoluminescence spectra were collected on single crystalline samples using a Horiba Jobin-Yvon Fluorolog-3 fluorometer, whereas radioluminescence spectra were obtained at the Physical, Chemical, and Nano Sciences Center at Sandia National Labs-New Mexico using a fiber-optic coupled spectrometer and 2.5 MeV protons at a high current density of 500 nA/cm^2. No new radioluminescence bands were observed for complexes **1**-**5** upon successive irradiation doses, indicating the damage mechanism does not produce new luminescent species. Instead, the entire spectrum decreases uniformly with dose, indicating the differences in ion-beam induced luminescence (IBIL) are intrinsic to the MOF structures and not due to radiation damage.

3. Results and Discussion.

Two classes of structures were chosen for the present study, the first group belonging to the so-called 'isoreticular' MOF (IRMOF) family, named on the basis of their identical cubic framework topologies.[5] Complex **1** (IRMOF-10) is the first structure of this type, employing tetrahedral Zn_4O metal cluster nodes and $BPDC^{2-}$ linker groups, as shown in figure 2. This complex possesses large inter-linker distances of 15.44 Å, leading to a low-density porous framework with minimal intermolecular interactions. Complex **2** (IRMOF-8) is another member of this family, employing NDC^{2-} linker groups (figure 3) in place of $BPDC^{2-}$. A reduced inter-linker separation of 12.61 Å is observed in **2**, as expected for the shorter NDC^{2-} struts. Complexes **3** and **4** belong to the MIL (Materials of Institut Lavoisier) family of materials and are comprised of linear chains of Al(OH) metal clusters connected into a 3-D framework by NDC^{2-} linkers, as shown in figure 4.[6,7] These related structures are remarkable in that they undergo a reversible structural transformation that is dependent upon activation conditions. The 'open' complex **3** possesses removable guest $CHCl_3$ solvent molecules in the open 1-D channels, transforming to the nonporous 'closed' complex **4** upon heating and evacuation. Dramatic structural changes are associated with this accordion-like transformation, as described by reduced interchromophore distances and Al-Al-Al angles (α) for **4** shown in figure 4 (bottom). Complex **5** is identical to **2**, with the exception of the electron donor N,N-diethylaniline trapped within the pores.

Figure 5 shows the photoluminescence and IBIL spectra for complex **1**, revealing a large 65 nm Stokes shift and nearly superimposable photoluminescence/IBIL emission spectra. The structureless emission band at ~400nm is not surprising due to free rotation about the C_{phenyl}-C_{phenyl} bond in $BPDC^{2-}$. Photoluminescence decay measurements on **1** reveal a bi-exponential decay with decay times of τ_1=5.4ns (58%) and τ_2=15.0ns (42%). Markedly different luminescence spectra were obtained for complex **2** (figure 6), including the observation of vibronic structure in both photoluminescence and IBIL spectra, as well as an intense new IBIL emission peak at 476nm. This feature is reminiscent of the previously reported isostructural SDC-based MOF, and may be attributed to the formation of excimer species upon ion-beam irradiation. These combined results for **1** and **2** may be rationalized by considering the geometry of $BPDC^{2-}$ and NDC^{2-} in their respective ground and excited states. $BPDC^{2-}$ possesses a twisted orientation in the ground state and a planar geometry in the excited state, leading to a low probability for the formation of excited state dimers.[8] In contrast, SDC^{2-} and NDC^{2-} readily form excimer species upon irradiation due to intermolecular π-π interactions in both the ground and excited state.[9,10] The photoluminescence decay for **2** was also measured, resulting in a biexponential decay (λ=383nm) with τ_1=4.7ns (96%) and τ_2=16.9ns (4%), representing a remarkable rate enhancement compared to naphthalene molecular crystals (τ_1=18ns (7%) and τ_2=82ns (93%)).[11]

Complexes **3** and **4** were also studied via photo- and radioluminescence spectroscopy to confirm the above assignment of the red-shifted IBIL peak. The open-framework complex **3** possesses minimal intermolecular interactions, leading to photoluminescence spectra that are comparable to free H_2NDC monomer in dilute solution. Significantly different spectral characteristics were observed upon conversion to the nonporous closed complex **4**, as indicated by the single red-shifted photoluminescence excimer emission (figure 7). No evidence for monomer emission is observed in

either the photoluminescence or IBIL spectra, suggesting efficient energy transfer between interacting NDC^{2-} groups. Interestingly, the IBIL and photoluminescence emission spectra for **4** are nearly superimposable, confirming the excimer assignment of this peak.

The infiltrated complex **5** was also synthesized to further demonstrate the ability to tune the luminescence properties of MOF-based scintillators. The electron donor N,N-diethylaniline (DEA) was chosen as an extrinsic dopant due to its ability to form strong charge-transfer complexes with aromatic acceptor molecules. This intense and structureless photoluminescence charge-transfer (exciplex) band is evident at 559 nm in figure 8, whose appearance is associated with a concomitant decrease in the monomer emission at ~400nm. The very large 160nm exciplex Stokes shift attests to a large degree of internal reorganization in the excited state, owing to the large geometrical changes that occur in DEA upon conversion from a planar radical cation structure to a pyramidal neutral structure.[12] Furthermore, the above observations indicate the efficient formation of a contact radical ion pair upon photoirradiation, leading to fluorescence emission that represents a nonadiabatic back electron transfer that regenerates the neutral NDC^{2-} and DEA starting materials. Inspection of the IBIL spectrum for **5** reveals three unique spectral features, corresponding to monomer emission at 400nm, excimer emission at 475nm, and exciplex emission at 545nm. This provides a vivid demonstration of how the synthetic and structural flexibility of MOFs leads to new, tunable sources of emission.

4. Conclusions.

The above studies are a part of ongoing efforts to understand the specific factors that control the luminescence yield and timing of scintillators. MOFs have been chosen as a molecular-level platform from which to study these phenomena due to a host of particularly attractive properties, including: well-defined crystalline structures, high thermal and chemical stability, fast timing characteristics, modular and controllable synthetic procedures, large permanent porosities for hosting infiltrated materials, scintillation yields comparable to commercial plastic and organic scintillators, and a high tolerance to radiation damage. We are developing practical materials and new methods for particle discrimination, which will be published separately.

References:

1) Ockwig, N.W.; Delgado-Friedrichs, O.; O'Keeffe, M.; Yaghi, O.M. *Acc. Chem. Res*. **2005**, 38, 176.
2) Yaghi, O.M.; O'Keeffe, M.; Ockwig, N.W.; Chae, H.K.; Eddaoudi, M.; Kim, J. *Nature*, **2003**, 423, 705.
3) Surble, S.; Serre, C.; MellotDraznieks, C.; Millange, F.; Ferey, G. *Chem. Commun*. **2006**, 284.
4) Doty, F.P.; Bauer, C.A.; Skulan, A.J.; Grant, P.G.; Allendorf. M.D. *Adv. Mater*. **2009**, 21, 95.
5) Eddaoudi, M.; Kim, J.; Rosi, N.; Vodak, D.; Wachter, J.; O'Keeffe, M.; Yaghi, O.M. *Science* **2002**, 295, 469.
6) Loiseau, T.; Serre, C.; Huguenard, C.; Fink, G.; Taulelle, F.; Henry, M.; Bataille, T.; Ferey, G. *Chem. Eur. J*. **2004**, 10, 1373.
7) Senkovska, I.; Hoffmann, F.; Froba, M.; Getzschmann, J.; Bohlmann, W.; Kaskel, S. *Micropor. Mesopor. Mater*. **2009**, 122, 93.
8) Liu, X-H.; Satoh, N.; Kugo, G-I.; Abe, K.; Shigenari, T.; Narisawa, T. *J. Phys. Soc. Jpn*. **1999**, 68, 284.
9) Brocklehurst, B.; Bull, D.C.; Evans, M.; Scott, P.M.; Stanney, G. *J. Am. Chem. Soc*. **1974**, 97, 2977.
10) Azumi, T.; Azumi, H. *Bull. Chem. Soc. Jpn*. **1966**, 39, 2317.
11) Selvakumar, S.; Sivaji, K.; Arulchakkaravarthi, A.; Balamurugan, N.; Sankar, S.; Ramasamy, P. *J. Cryst. Growth* **2005**, 282, 370.
12) Cosa, G.; Chesta, C.A. *J. Phys. Chem. A* **1997**, 101, 4922.

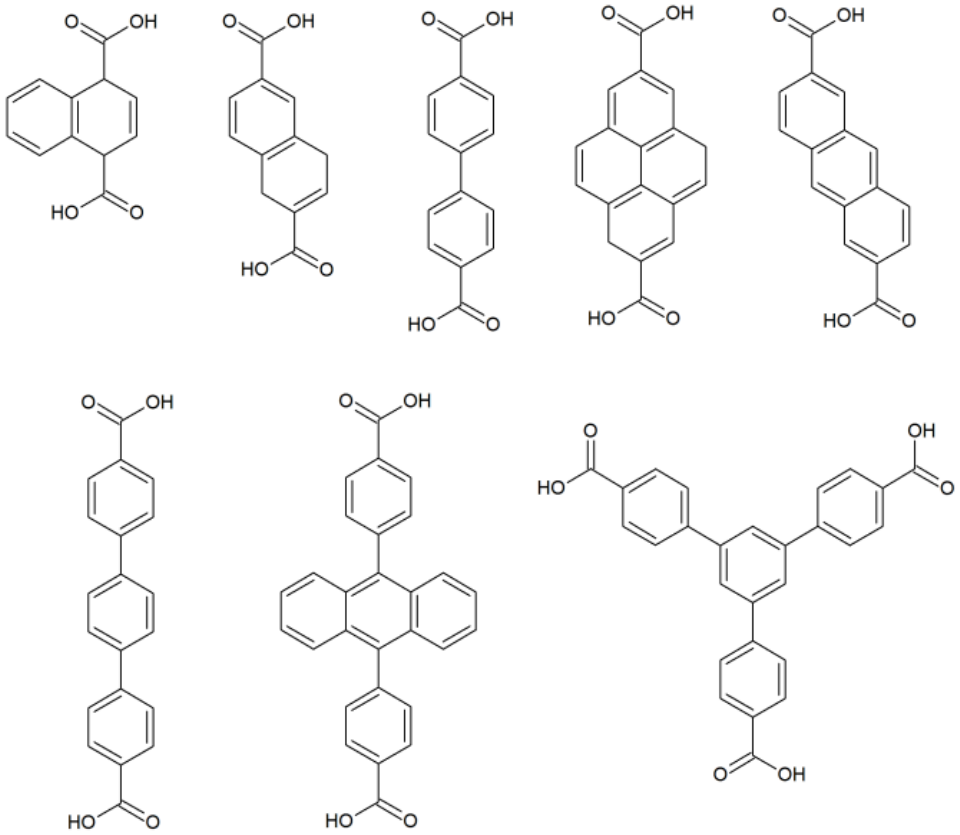

Figure 1. Representative sampling of scintillating linker groups used in MOF synthesis.

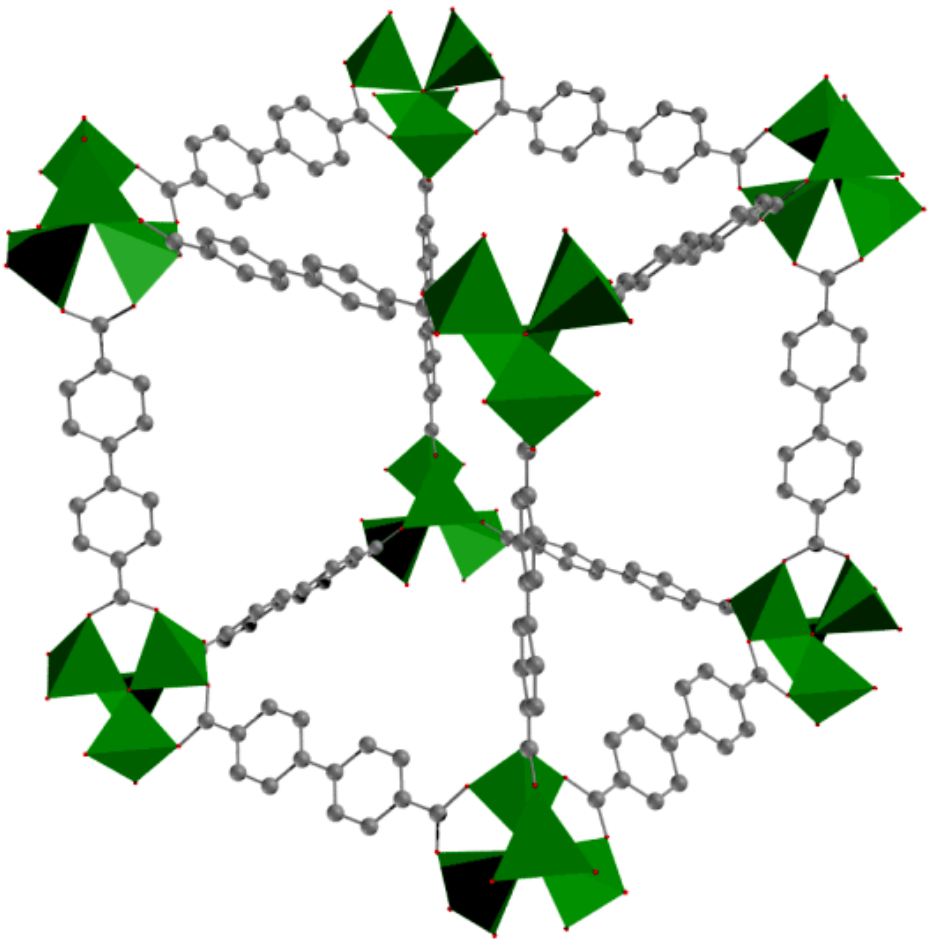

Figure 2. Molecular structure of a repeating structural subunit in complex **1**.

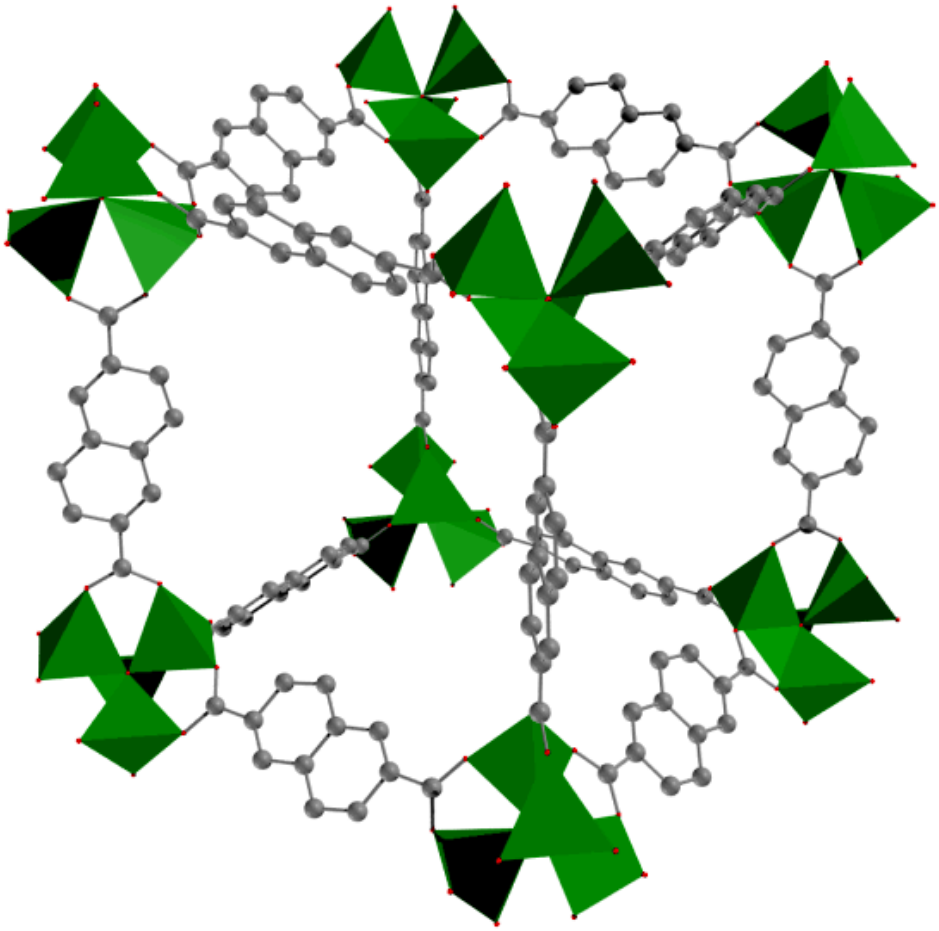

Figure 3. Molecular structure of a repeating structural subunit in complex **2**.

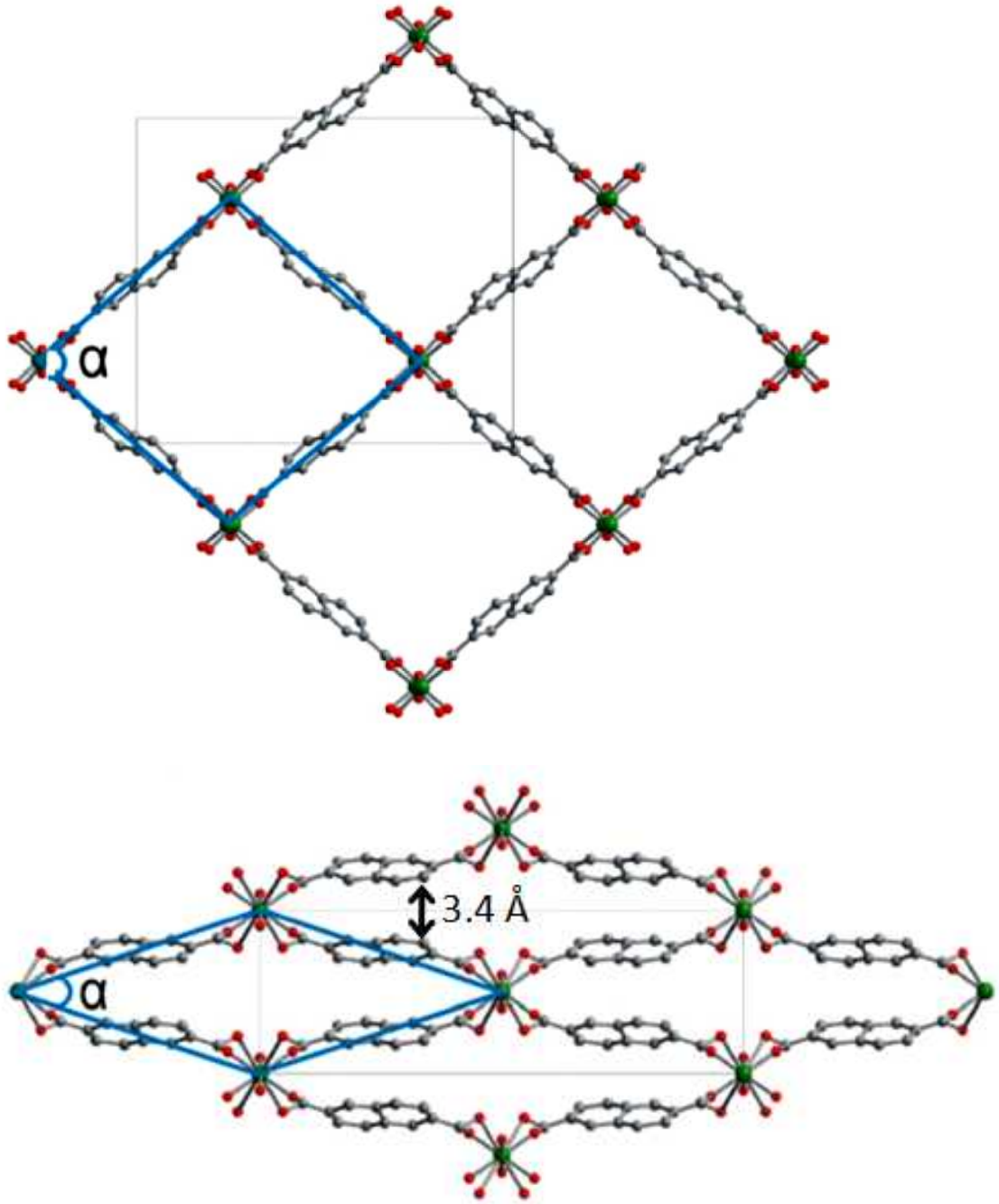

Figure 4. Molecular structures of complexex **3** (top) and **4** (bottom). The opening angles (α) are 87° and 34° for **3** and **4**, respectively.

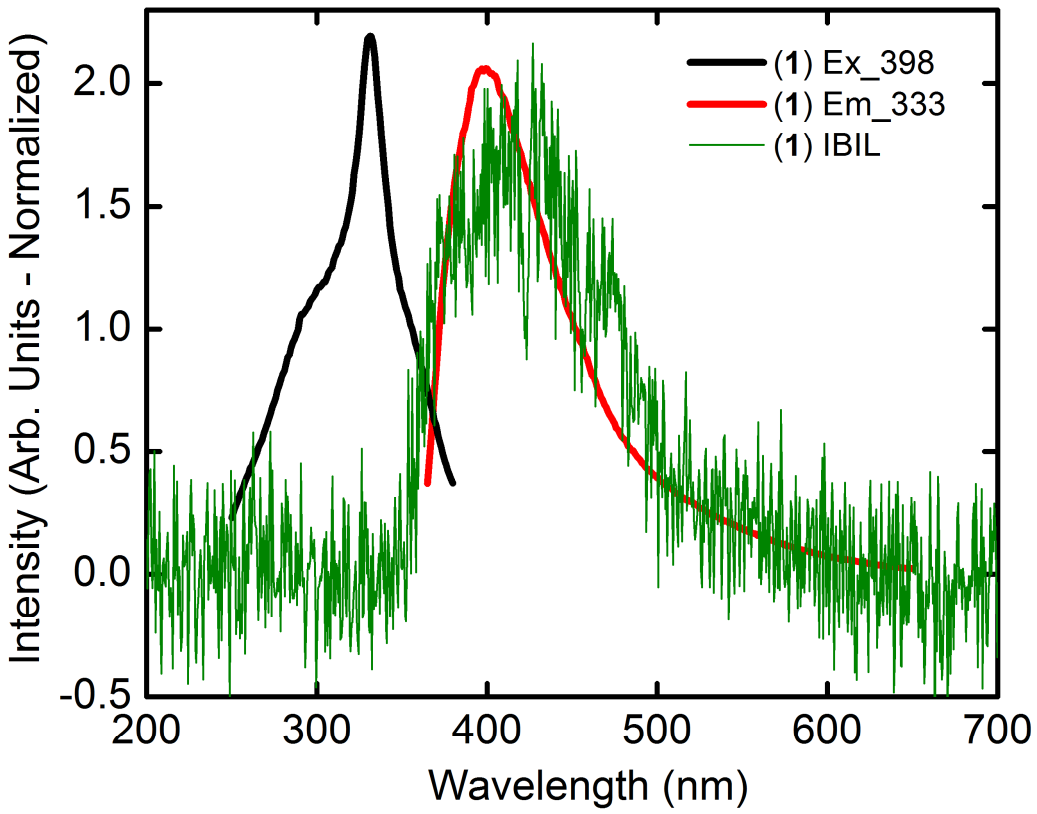

163
164 Figure 5. Photoluminescence and IBIL spectra for complex **1**.

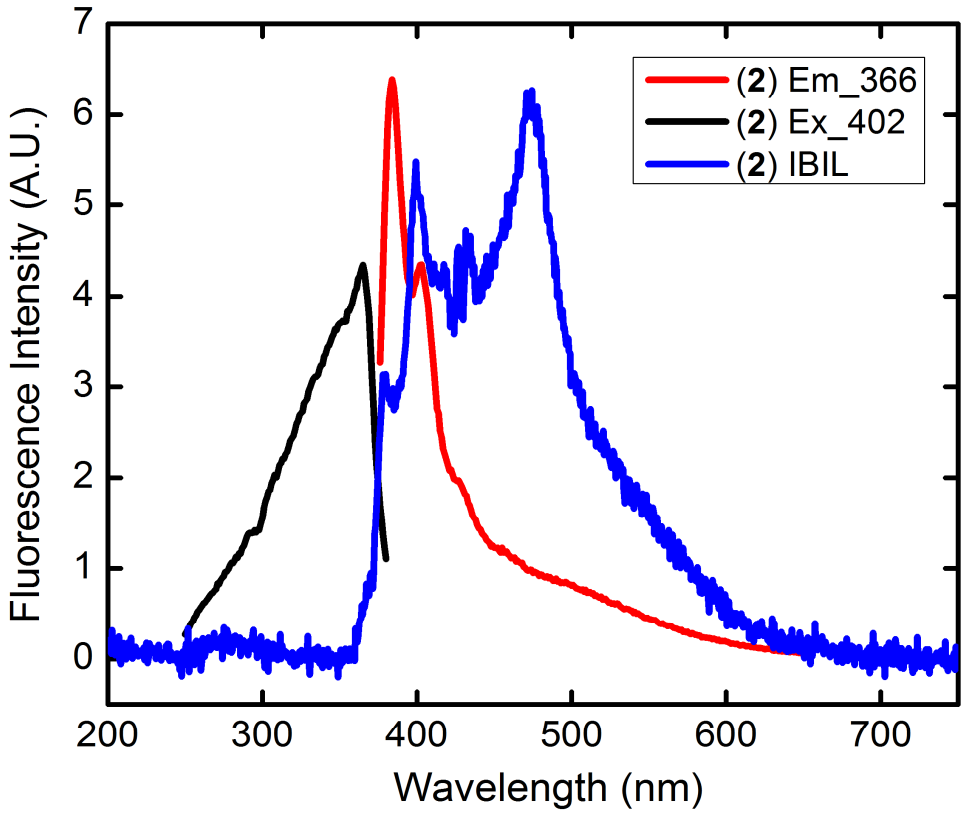

Figure 6. Photoluminescence and IBIL spectra for complex **2**.

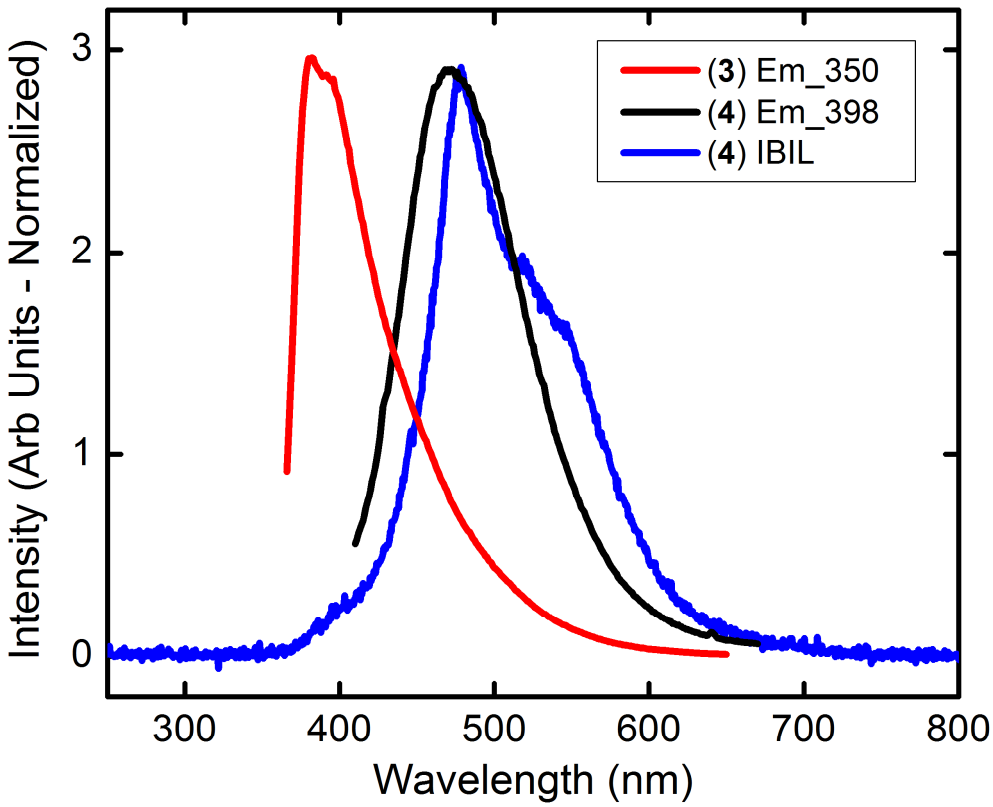

Figure 7. Photoluminescence and IBIL emission spectra for complex **4**. The monomeric photoluminescence emission for **3** is provided for comparison.

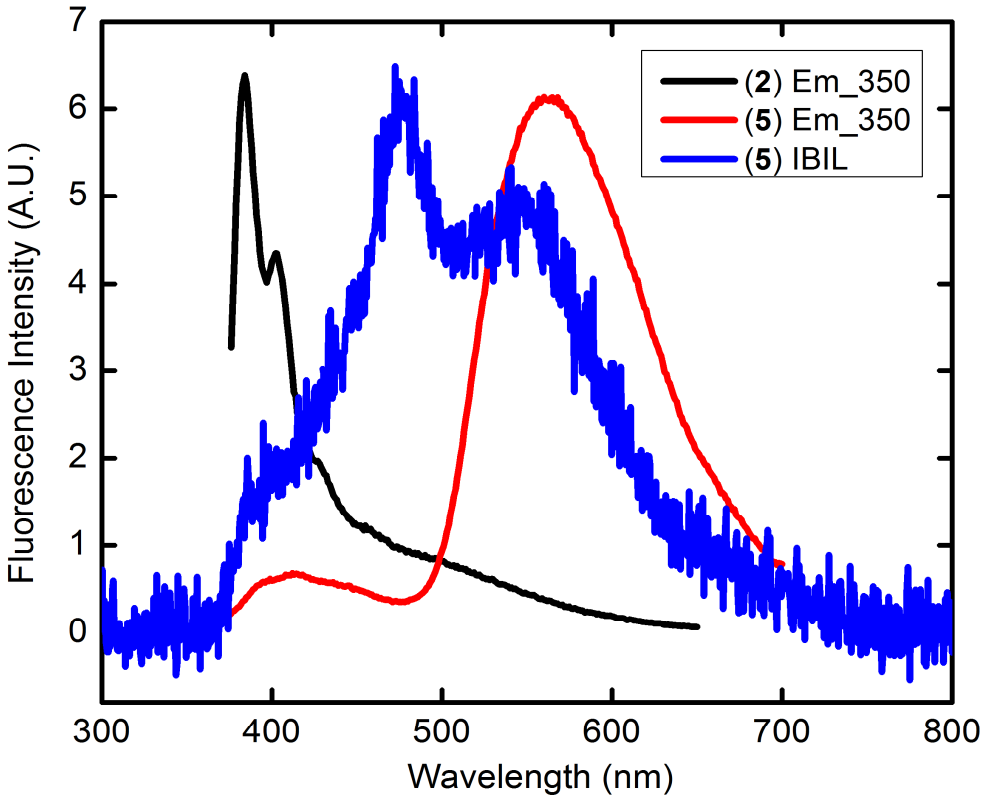

Figure 8. Photoluminescence and IBIL emission spectra for complex **5**. The monomeric photoluminescence emission for **2** is provided for comparison.